AFM and UFM Surface Characterization of Rubber-Toughened Poly(methyl methacrylate) Samples

K. PORFYRAKIS, O. V. KOLOSOV, H. E. ASSENDER

Department of Materials, University of Oxford, Parks Road, Oxford OX1 3PH, United Kingdom

Received 22 December 2000; accepted 28 February 2001

ABSTRACT: The microstructure of a series of injection-molded and extruded rubber–toughened poly(methyl methacrylate) (RTPMMA) samples was investigated. Atomic force microscopy (AFM) and ultrasonic force microscopy (UFM) were used to study surface topography and local elastic properties. AFM topography measurements combined with UFM can reveal the distribution and orientation of the rubber particles in the PMMA matrix. UFM, in particular, reveals the core–shell structure of the particles as well as the presence of particles immediately under the surface, otherwise invisible. In some cases the particles appear to be covered by a thin PMMA layer, whereas in other cases they appear to have broken, thereby exposing parts of their internal structure. Generally, the particles are elongated in the skin region of the injection-molded samples. On the other hand, the particles in the surface region of the extruded samples appear to be almost spherical. The observed difference is attributed to the fountain flow phenomenon, which takes place during injection molding. © 2001 John Wiley & Sons, Inc. J Appl Polym Sci 82: 2790–2798, 2001

Key words: rubber-toughened polymer; RTPMMA; UFM; particle elongation

INTRODUCTION

There is a broad range of analytical techniques that may be used to characterize microstructures in polymeric materials. Among the physical characterization methods, two modes of scanning force microscopy (SFM), with its family of techniques including atomic force microscopy (AFM) and ultrasonic force microscopy (UFM), are rapidly gaining prominence. SFM can resolve details to the subnanometer size scale, matching or even exceeding the capabilities of more traditional microscopic techniques, as shown in Table I.[1]

Rubber-toughened acrylics are widely used for molded, formed, and extruded components. Fracture resistance of these toughened materials is largely controlled by the dispersion of the rubber particles, their internal structure, and the adhesion between the particles and the matrix. Particle size distribution is important, given that it is known that there is often an optimum "window" of particle sizes for each system. Toughening elements that agglomerate or elongate during processing may reduce the effect of their toughening on the resulting material. This is particularly true close to the surface of the sample. SFM allows us for the first time to closely characterize rubber particle size, shape, and distribution as well as internal morphology, to some extent, immediately adjacent to the surface of a molding or extrudate. The technique requires minimal sample preparation, leaving the morphology undisturbed prior to examination.

The present study involves the use of AFM and UFM for microstructural investigation of rubber-

Correspondence to: H. E. Assender.

Contract grant sponsor: EPSRC; INEOS Acrylics (Wilton, UK).

Journal of Applied Polymer Science, Vol. 82, 2790–2798 (2001)

© 2001 John Wiley & Sons, Inc.

Table I Example of Morphological Characterization Techniques and the Length Scales of the Structure They Characterize

Characterization Technique	Size Range
Light scattering (LS)	200 nm–200 μm
Optical microscopy (OM)	200 nm–200 μm
Scanning electron microscopy (SEM)	4 nm–4 mm
Scanning force microscopy (STM, AFM, etc.)	0.2 nm–0.02 mm
Transmission electron microscopy (TEM)	0.2 nm–0.2 mm
Small-angle X-ray scattering (SAXS)	1.5–100 nm
Wide-angle X-ray scattering (WAXS)	0.01–1.5 nm

toughened poly(methyl methacrylate) (RTPMMA) samples. The toughening particles, prepared by emulsion polymerization, consist of three radially alternating rubbery and glassy layers, with the outer layer always being glassy polymer. These particles are crosslinked during their formation so that they maintain their morphology and size during blending with PMMA. Figure 1 shows schematically the size and internal structure of a toughening particle.[2] Samples of acrylic/rubber blends were prepared by extrusion and injection molding, the most commonly used polymer processing techniques.

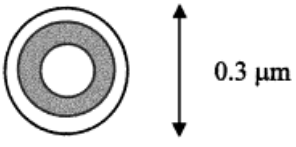

Figure 1 Schematic diagram of a three-layer toughening particle, showing its size and internal structure. The rubber layer is displayed dark and glassy layers light.

EXPERIMENTAL

Atomic Force Microscopy (AFM)

Scanning force microscopy (SFM) is the general name given to a variety of microscopy techniques that have a basic common principle of operation. The common feature is that the image is produced by scanning a probe on the surface of the specimen, with contrast resulting from some mechanical interaction between the tip and the surface.

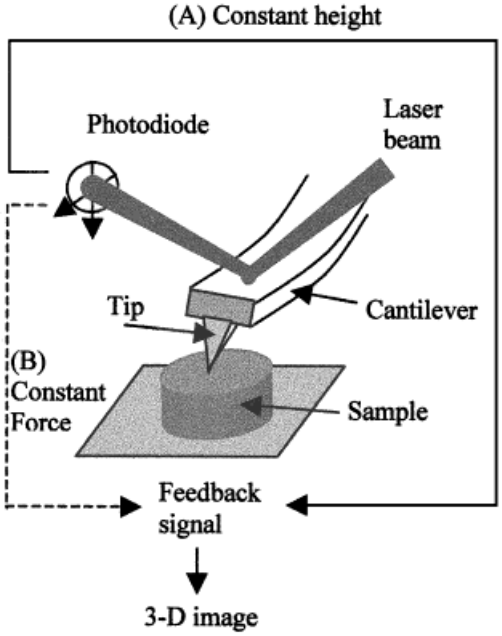

Figure 2 Schematic of a typical AFM.

Atomic force microscopy (AFM) is currently one of the most important of this family of techniques for studying of nanoscale morphology of surfaces. The probe or tip, usually a few micrometers long and often less than 100 Å in diameter, is mounted on a cantilever 100–200 μm long. A set force between the tip and sample surface causes the cantilever to deflect or bend. The direction of a laser beam reflected off the back of the cantilever is used to probe the deflection of the cantilever as it scans the sample surface; thus, an image of the surface topography may be generated. Figure 2 shows a schematic representation of the principle of operation of AFM. A more detailed description and an in-depth theoretical analysis of AFM can be found elsewhere.[1,3]

Ultrasonic Force Microscopy (UFM)

An important modification of AFM is ultrasonic force microscopy (UFM). UFM is a novel technique developed during the last decade by Kolosov and Yamanaka,[4,5] which combines the high spatial resolution of AFM with sensitivity to surface elastic and adhesive properties. It is suitable for imaging a wide range of materials, from hard ceramics to soft polymers as well as composite materials such as RTPMMA. An ultrasonic vibration (in the MHz range), at frequencies much

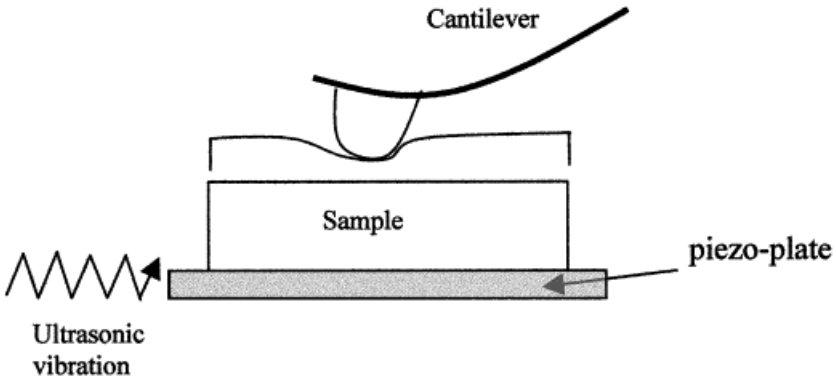

Figure 3 Schematic of operation of UFM. The application of an ultrasonic vibration causes the tip to indent itself into the sample.

higher than the primary cantilever resonance, is applied to a piezo-plate underneath the sample. As a result, the tip does not vibrate with the sample but, rather, is cyclically indented into the sample, as shown in Figure 3. Friction is considerably reduced in the presence of high-frequency vibration, making this technique attractive for polymer samples that may easily be damaged by the tip.[6]

The tip–sample distance is modulated within the nonlinear regime of the tip–sample interaction force, resulting in a net additional force on the tip, the "ultrasonic force." This may be understood as the average force experienced by the tip during an ultrasonic period; hence, the cantilever experiences an additional displacement whose magnitude depends on the details of the tip–sample force. Materials with different elastic or adhesive properties will cause a different response of the cantilever to the applied vibration. It is not in the scope of the present study to analyze further the theoretical background of UFM; a substantial number of investigations regarding the underlying physics and principle of operation of UFM were previously published in the scientific literature.[4–13] Nevertheless, some new and exciting results obtained using UFM are presented here for a series of rubber-toughened PMMA samples.

Samples and Experimental Method

An injection-molding machine (model DEMAG D40–151) was used to produce RTPMMA samples 120 × 10 × 4 mm (25% w/w in rubber particles), under a range of processing conditions.

A Rosand RH7–2 advanced rheometer (single barrel, twin-bore system) was used to prepare samples, simulating the extrusion process. Circular dies of two different sizes [16 × 1 and 32 × 2 mm (length × diameter)] were used.

A Park Scientific Instruments Autoprobe CP atomic force microscope was used to acquire AFM topography images in the contact mode. Park Scientific silicon and gold-coated triangular ultralevers were used (types UL 06 B and UL 06 A, respectively). Their properties are shown in Table II.

The Autoprobe CP system was modified to acquire the UFM signal simultaneously with topography. The samples were mounted on a ceramic piezotransducer using a thin layer of crystalline salol (phenyl salicilate) before mounting on the AFM. Vibrations with frequencies up to several MHz were excited in the sample. The ultrasonically induced normal deflection of the tip is relayed through a lock-in amplifier and displayed on a two-channel oscilloscope. A schematic of the experimental UFM setup is shown in Figure 4.

RESULTS AND DISCUSSION

Specimens from the injection-molded and "extruded" samples were used for surface AFM and

Table II Characteristics of the Cantilevers Used for AFM and UFM

Cantilever Type	UL 06 A	UL 06 B
Cantilever length	180 μm	180 μm
Cantilever width	18 μm	38 μm
Cantilever thickness	0.6 μm	1 μm
Radius of curvature	<50 nm	10 nm
Force constant	0.05 N/m	0.40 N/m
Resonant frequency	22 kHz	45 kHz

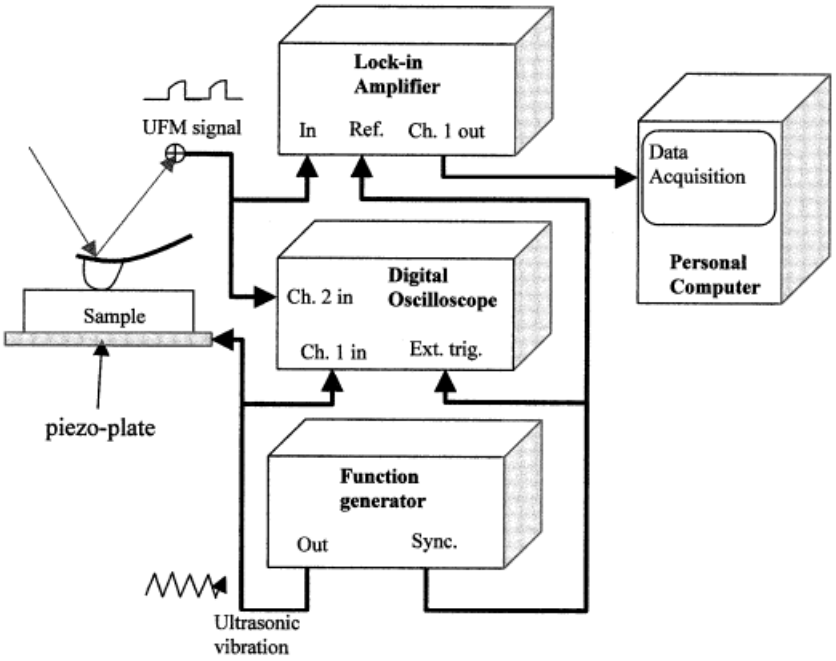

Figure 4 Schematic of the experimental UFM setup.

UFM characterization. The surface of the injection-molded bars was mapped along their width and their length in an attempt to determine the shape, size, and dispersion of the rubber particles. As the sample surface is imaged in each case, no further sample preparation such as sectioning was carried out. Figures 5 and 6 show AFM topography and UFM images of the injection-molded samples at different locations on the sample surface. In each case, the pairs of images were taken simultaneously at the same position on the sample surface.

The first conclusion one can draw is that the sample surface is not flat in the nanometer scale. AFM topography images reveal the presence of "bumps" and cavities. These features are attributed to the presence of the rubber particles embedded in the sample surface. This conclusion is verified by UFM characterization. UFM images give more information on the rubber-toughened microstructure because of the sensitivity of the technique to surface elastic and adhesive properties. In this case, because of the substantial difference in stiffness between rubber particles and the PMMA matrix, it is believed that elastic properties provide the main contribution to the UFM signal. A comparison was made[14] of a number of different scanning force microscopy techniques for imaging these surfaces, and contrast from the rubber particles was achieved in each case. In the UFM image, the compliant material appears darker, whereas stiffer material appears brighter. UFM images can also reveal the presence of rubber particles immediately under the surface, as shown in Figure 5 (e.g., at the position marked within circle 1). These particles are invisible in the AFM images. This provides evidence that UFM can be used to probe the properties of the subsurface without any significant damage to the sample.

The shape, size, and orientation of the rubber particles can also be analyzed by combining AFM with UFM. It is generally observed that the rubber particles are well oriented with the flow direction. UFM images, in particular, reveal the shape of the rubber particles. It is evident that the particles are quite elongated close to the surface, as suggested by the fountain flow phenomenon depicted schematically in Figure 7.[15] During the filling stage of injection molding and in the vicinity of the flow front, the fluid spills outward toward the walls. This flow pattern, combined with the high stresses and thermal gradients present, causes the rubber particles to elongate as they approach the cold walls. Because of the low wall temperature, the melt in this vicinity solidifies rapidly, creating a solid skin next to the walls; hence, the particles are trapped, retaining their shape and orientation.

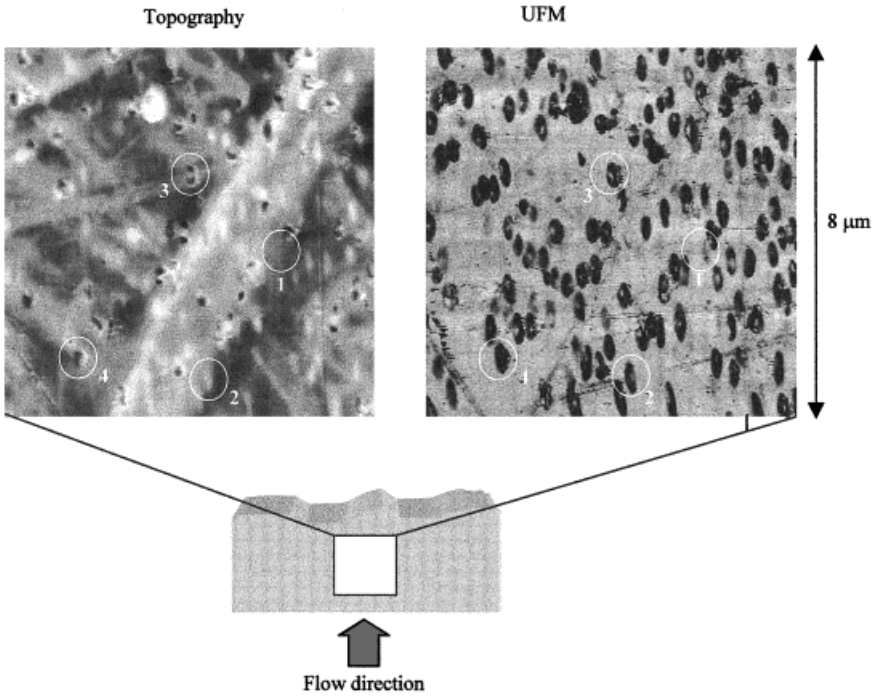

Figure 5 AFM topography (left) and UFM (right) images of the surface of an injection-molded bar taken from an area close to the gate where the polymer melt enters the mold cavity. The flow is vertical. The two images of the same sample area were taken simultaneously. Circles 1–4 identify examples of rubber particles, as discussed in the text.

Height-profile analysis was carried out to calculate the particles' contour and size, an example of which is shown in Figure 6. The height of the observed bumplike features varies typically from 50 to 150 nm. The particles form ellipsoids with significant elongation. The eccentricity e of the projected ellipses varies from 0.70 to 0.95, and is calculated by the following equation:

$$e = \left[1 - \left(\frac{b}{a}\right)^2\right]^{1/2}$$

where a is the major axis and b is the minor axis. The eccentricity of an ellipse can vary between the values of 0 (for a circle) and 1 (for a parabola). The length (major axis) of the particles, on average, varies between 600 and 900 nm.

Closer investigation of the AFM and UFM images coupled with height-profile analysis can reveal important information on the internal structure of the particles. Figure 8 shows a schematic of the different particle structures encountered in Figures 5 and 6. In some cases the particles are covered by a thin layer of PMMA matrix [Fig. 8(a)]. Therefore, they appear as bumplike features in the AFM images. Their internal structure, however, can still be revealed in the UFM images, as shown in Figure 5 (e.g., at the position marked within circle 2). In other cases the particles seem to have "broken," thereby exposing some part of their internal structure [Fig. 8(b) and (c)]. An example of what is thought to be the structure illustrated in Figure 8(b) can be seen in the height-profile analysis images of Figure 6 and in Figure 5 (e.g., at the position marked within circle 3). The position marked within circle 4 in Figure 5 shows an example of what is thought to be the structure illustrated in Figure 8(c).

The extent of this phenomenon depends on several factors. It is possible that the particles were broken during the sample production. Often the mold surface is contaminated or some defect is present. Additionally, the samples are ejected from the mold cavity rather violently by the ejection pins. These conditions are almost certain to introduce some damage to the sample surface and hence the particles themselves. Another possibility is that damage to the particles is caused by the

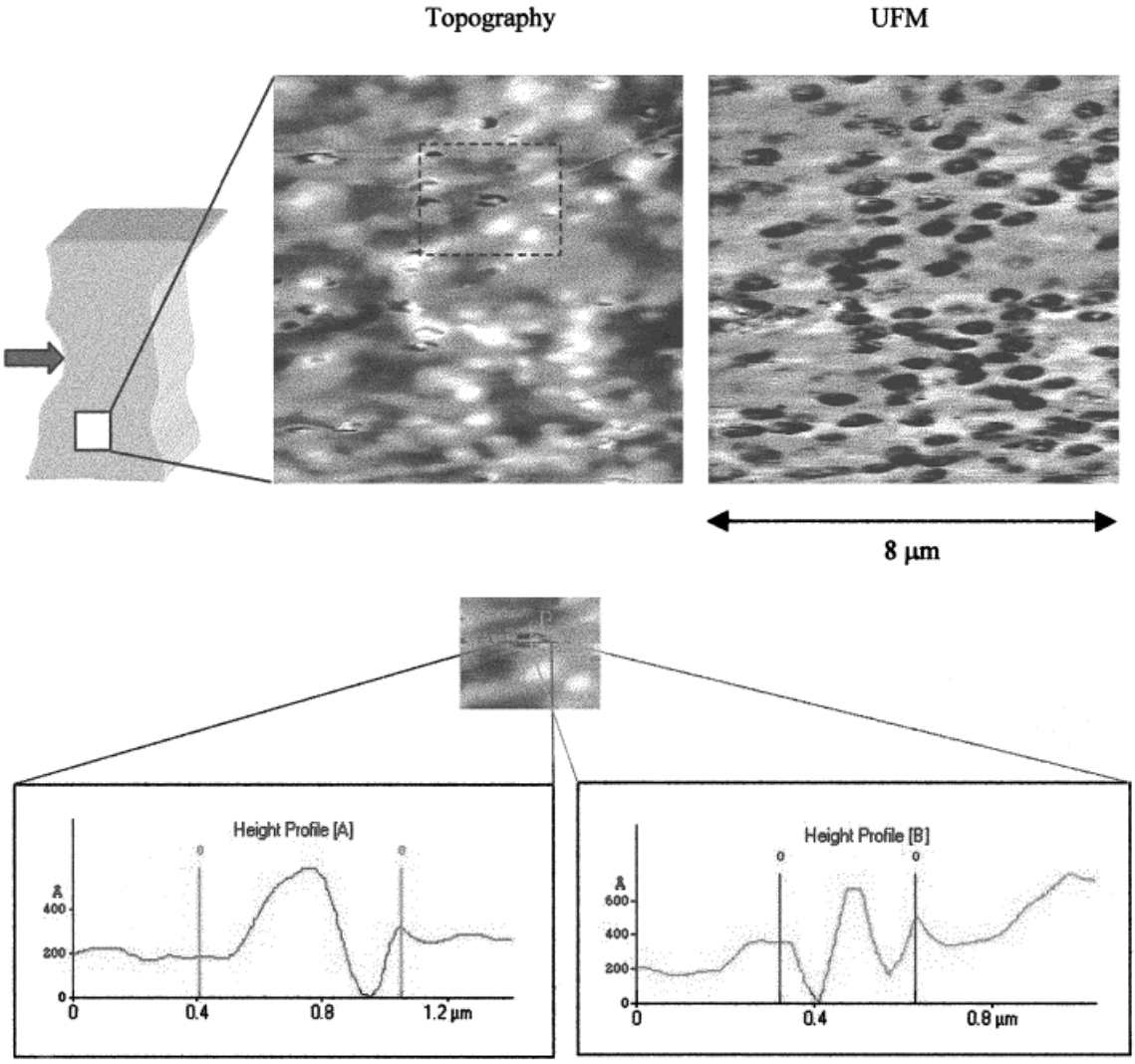

Figure 6 AFM topography (left) and UFM (right) images taken from an area on an injection-molded bar further down the flow direction than that in Figure 5. The flow direction is horizontal. Elongation of the rubber particles is evident. The image at the bottom shows height-profile analysis carried out over a single particle (highlighted by the dashed box in the AFM image) to establish its contour and size.

tip while scanning the sample surface. It is good practice to retain a slow scanning speed for the tip. However, tip-induced damage to the particles is not completely inescapable. In particular, extensive protrusion of a particle or poor localized adhesion between a particle and the PMMA matrix could both facilitate the "slicing" of the particle by the tip.

The surface of extruded samples was also analyzed using AFM and UFM, as shown in Figure 9. Given the smoothness of the samples, the images are particularly clear. Even AFM alone can give good information on the dispersion of the particles; however, the internal structure of the particles can be seen only in the UFM image. It can be observed that the rubber particles do not tend to agglomerate but are relatively well distributed in the matrix. Another important observation one can make is that the particles are almost spherical, in direct contrast with the injection-molding process, in which the particles are substantially elongated in the skin region of the sample. This was confirmed by height-profile analysis of the particles in a manner similar to that illustrated in Figure 6. The reason for the spherical nature of the particles is that during extrusion the particles are allowed to relax as they exit the die before

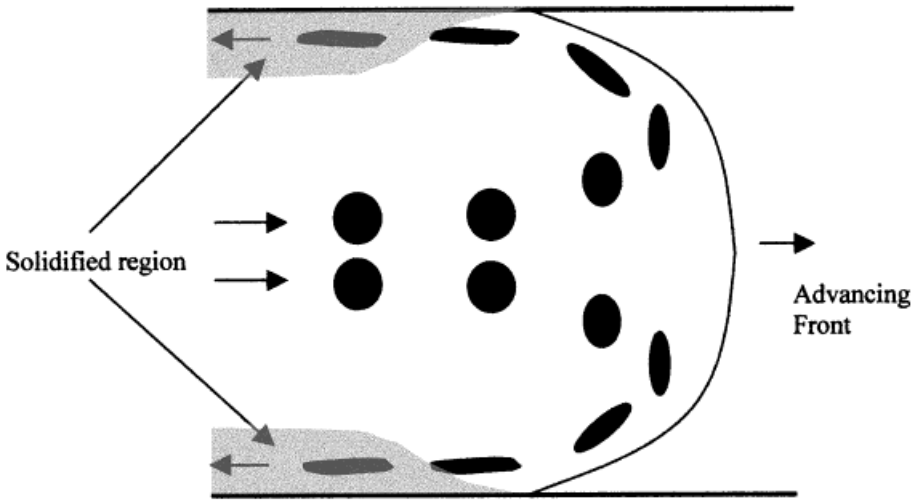

Figure 7 A schematic illustration of the fountain flow phenomenon of polymer injection molding showing the resulting observed elongation of the rubber particles close to the wall.

the surface is cooled in ambient temperature, as opposed to injection molding, where rapid surface cooling leads to the fountain flow phenomenon described earlier.

Overall, by studying the AFM and UFM images presented earlier, it can by postulated that, compared to the injection-molded samples, the extruded samples exhibit better dispersion and less elongation of the rubber particles. These observations are common to all the samples studied, covering a range of processing conditions such as barrel temperature, back pressure, and so forth. Our observations of the variation in morphology with the exact processing history, its effect on mechanical properties, and the computer simulation of such effects will be the subject of future publications.

The ability of AFM combined with UFM to display the elongation and dispersion of the rubber particles makes these techniques extremely useful when studying rubber-toughened polymers. Generally, the interrelationship between

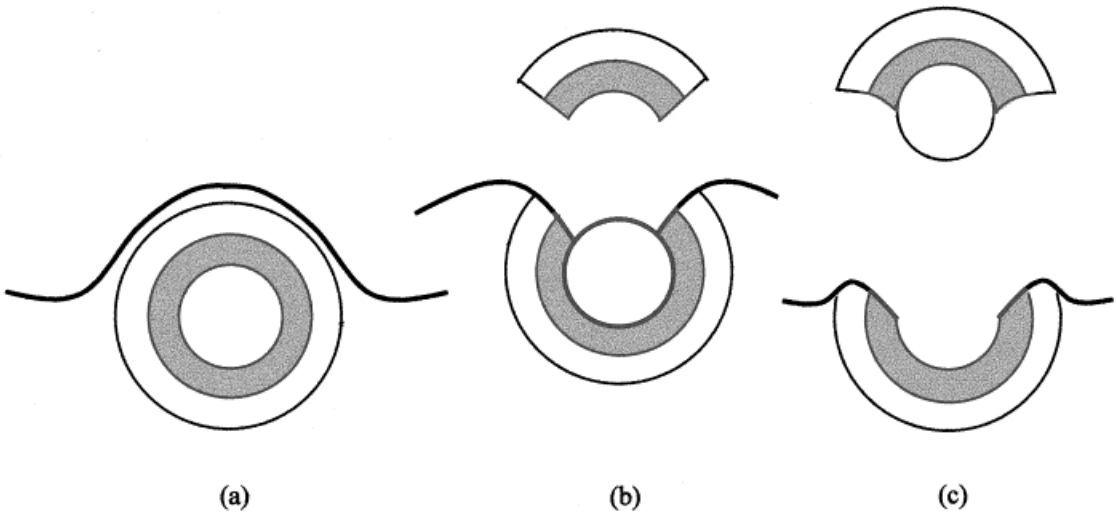

Figure 8 Schematic of the possible particle structures encountered by the AFM and UFM imaging. The particles may be completely covered by the PMMA matrix (a), or their core (b) or even the internal rubber layer (c) may be exposed at the surface.

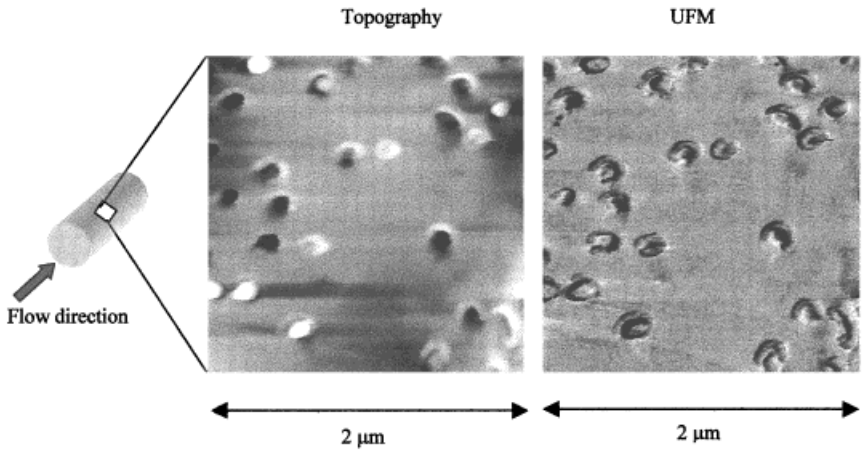

Figure 9 AFM topography (left) and UFM (right) images of the surface of an extruded sample. The rubber particle morphology is clearly observed with the particles showing no significant elongation.

processing conditions, microstructure, and mechanical properties has not yet been fully developed. The main reason is the complexity of a process such as injection molding and the large number of possible parameter combinations that can be used to produce a molded part. By studying the sample surface by AFM and UFM one can have an estimate of the rubber volume fraction in the skin region. It is known that impact fracture resistance increases with increasing volume fraction of rubber particles[16] and is usually accompanied by decreasing modulus and yield stress. Therefore, the microstructural information provided by AFM and UFM can be vital when investigating the fracture resistance of the sample, particularly when failure initiates at the surface. Thus, AFM and UFM can provide a useful link between processing conditions and mechanical properties.

AFM topography images of the injection-molded samples reveal the presence of bumps and cavities. These features are attributed to the rubber particles present on the sample surface. UFM images confirm this and reveal the presence of rubber particles immediately under the surface. More important, UFM reveals that the particles are quite elongated in the skin region. UFM coupled with height-profile analysis clearly reveals the core–shell structure of the particles. In some cases the particles appear to be sliced, exposing their internal rubbery layer or even their glassy core.

The surface of the extruded samples was also analyzed using AFM and UFM. Compared to the injection-molded samples, the extruded samples exhibit better dispersion and less elongation of the rubber particles.

CONCLUSIONS

A series of rubber-toughened poly(methyl methacrylate) (RTPMMA) samples were produced by extrusion and injection molding for examination with two modes of scanning force microscopy, atomic force microscopy (AFM) and ultrasonic force microscopy (UFM). UFM in particular, being sensitive to surface elastic and adhesive properties, clearly shows the morphology. AFM combined with UFM can be very informative on the rubber-toughened microstructure.

The authors thank EPSRC and INEOS Acrylics (Wilton, UK) for funding this project. In particular, Dr. Ian Robinson is gratefully acknowledged for provision of facilities and useful discussions. Many thanks to Gary Hunt and Ian Dargue for their guidance during the injection-molding experiments. Dave Stocks and Patricia Walker are also deeply acknowledged for their assistance during the rheology experiments. Finally, many thanks to Dr. Franco Dinelli for many valuable discussions.

REFERENCES

1. Sawyer, L. C.; Grubb, D. T. in Polymer Microscopy; Chapman & Hall, New York, 1996; Chapter 1.

2. Lovell, P. A.; McDonald, J.; Saunders, D. E. J.; Sherratt, M. N.; Young, R. J. in Toughened Plastics. I: Science and Engineering; Riew, C. K.; Kinloch, A. J., Eds.; Advances in Chemistry Series 233; American Chemical Society: Washington, DC, 1993.
3. Ratner, B. D.; Tsukruk, V. V., Eds. Scanning Probe Microscopy of Polymers; ACS Symposium Series 694; American Chemical Society: Washington, DC, 1998.
4. Kolosov, O.; Yamanaka, K. Jpn J Appl Phys 1993, 32, L1095.
5. Yamanaka, K.; Ogiso, H.; Kolosov, O. Appl Phys Lett 1994, 64, 178.
6. Dinelli, F.; Biswas, S. K.; Briggs, G. A. D.; Kolosov, O. V. Appl Phys Lett 1997, 71, 1177.
7. Dinelli, F. Ph.D. Thesis, University of Oxford, 1999.
8. Dinelli, F.; Assender, H. E.; Takeda, N.; Briggs, G. A. D.; Kolosov, O. V. Surf Interface Anal 1999, 27, 562.
9. Kolosov, O.; Ogiso, H.; Tokumoto, H.; Yamanaka, K. Nanostruct Quant Effects 1994, 31, 345.
10. Kolosov, O.; Briggs, A.; Yamanaka, K.; Arnold, W. Acoust Imaging 1996, 22, 665.
11. Warren, P. D.; Kolosov, O. V.; Roberts, S. G.; Briggs, G. A. D. Nanotechnology 1996, 7, 288.
12. Kolosov, O. Mater World 1998, 6, 753.
13. Dinelli, F.; Castell, M. R.; Ritchie, D. A.; Mason, N. J.; Briggs, G. A. D.; Kolosov, O. V. Philos Mag A Phys Condens Matter Struct Defect Mech Prop 2000, 80, 2299.
14. Cuberes, M. T.; Assender, H. E.; Briggs, G. A. D.; Kolosov, O. V. J Phys D Appl Phys 2000, 33, 2347.
15. Bucknall, C. B. Toughened Plastics; Applied Science Publishers: London, 1977; Chapter 11.
16. Lovell, P. A.; McDonald, J.; Saunders, D. E. J.; Sherratt, M. N.; Young, R. J. Plast Rubber Compos Process Appl 1991, 16, 37.